17th World Conference on Earthquake Engineering, 17WCEE

Sendai, Japan - September 13th to 18th 2020

Influence of strong ground motion of the 2011 Tohoku and 2016 Kumamoto Earthquake on the uplift of isolators of base isolated high-rise buildings

Y. Ikeda[(1)]

[(1)] *Assoc. Prof., Dept. of Social Design Engineering, Architecture and Civil Engineering and Disaster Prevention Course, National Institute of Technology, Kochi College, Dr. Eng., yikeda@ce.kochi-ct.ac.jp*

Abstract

The two office of base isolated building observed the strong motion records in the 1995 Hyogo Earthquake. The response acceleration of the horizontal component of the record has decreased compared with the horizontal acceleration component of the ground motion. After the earthquake, base isolated buildings have been designed for apartments, offices and hospitals, but predominantly for apartment buildings. Influenced by rising land prices, the height of isolated apartment buildings in large Japanese cities in Japan has risen from 10 to 15 stories, resulting into a larger aspect ratio for especially these types of base isolated structures.

In this study, the intensity of two horizontal and one vertical component on the uplift of isolators in large aspect ratio base isolated apartment buildings is quantitatively evaluated by using strong motion data of the 2011 Tohoku and the 2016 Kumamoto Earthquake.

Under strong motion, fluctuation axis force by overturning moment of the horizontal motion acts on the isolator in span direction. If the axis force of the vertical motion adds to the fluctuation axis force, an excessive uplift is generated in the isolator, increasing the risk for isolator damage. Tension stiffness of isolators is considerably smaller than their compression stiffness. When uplift is generated in an isolator, and the allowable tensile strength is exceeded, nonlinear behavior is shown. Therefore, structural designers are addressing this issue by trying to avoid uplift in isolators.

In the 2013 symposium of the Association of the Japan Society of Seismic Isolation (JSSI), an uplift case with large aspect ratio was reported for a base isolated university office building, located 400km west of the hypocenter. It is important to pay attention to the structural design of large aspect ratio base isolated buildings. After the Great East Japan disaster, isolator uplift in large aspect ratio base isolated apartment buildings against the long duration of seismic motion of the great earthquake of M8-9 class is the pressing issue.

The foreshock and the main shock of the 2016 Kumamoto Earthquake, each with a seismic intensity of 7 (Japan Meteorological Agency (JMA) Seismic Intensity Scale) acted on the buildings of Mashiki Town in Kumamoto Prefecture. Such strong ground motion in two consecutive occasions was not expected and not implemented in the seismic design of the buildings. Ground motion intensity during the 2 - 4 seconds predominant period was high in the 2016 Kumamoto Earthquake. This predominant period is corresponding to the first fundamental period band at the earthquake in base isolated buildings. When such strong ground motion acts on base isolated buildings, there is a high risk that isolators are pulled and that buildings collide with retaining walls. Scratch pad examination of the movement between the base and the building of a hospital in Aso City during the main shock of the 2016 Kumamoto Earthquake showed a maximum double amplitude of 92 cm and a maximum single amplitude of 46 cm. Earthquake resistance measures for base isolated buildings to withstand such strong ground motions scenarios are needed.

The intensity of seismic motion on two horizontal and one vertical component, which acted on large aspect ratio base isolated buildings, and which caused isolator uplift, was evaluated by using the strong motion records before the Great East Japan earthquake disaster. The evaluation index of efficiency was used for intensity evaluation and a quantitative difference between strong ground motion of inland earthquakes and plate boundary earthquakes was identified.

Keywords: the 2011 Tohuku Earthquake, the 2016 kumamoto Earthquake, strong ground motion, base isolated high-rise building, uplift of isolator

1. Introduction

The two office of base isolated building observed the strong motion records in the 1995 Hyogo Earthquake. The response acceleration of the horizontal component of the record has decreased compared with the horizontal acceleration component of the ground motion. After the earthquake, base isolated buildings have been designed for offices and hospitals, but predominantly for apartment buildings. Influenced by rising land prices, the height of isolated apartment buildings in large Japanese cities in Japan has risen from 10 to 15 stories, resulting into a larger aspect ratio for especially these types of base isolated structures.

According to the Association of the Japan Society of Seismic Isolation (JSSI), Fig-1 shows the number of base isolated buildings and isolated apartment buildings constructed in Japan from 1995 to 2017. On average, more than fifty base isolated apartment buildings are constructed every year. Fig-2 shows the number of constructed base isolated high-rise buildings in the same timeframe. As can be seen, the construction of base isolated high-rise buildings has increased sharply since the year 2000.

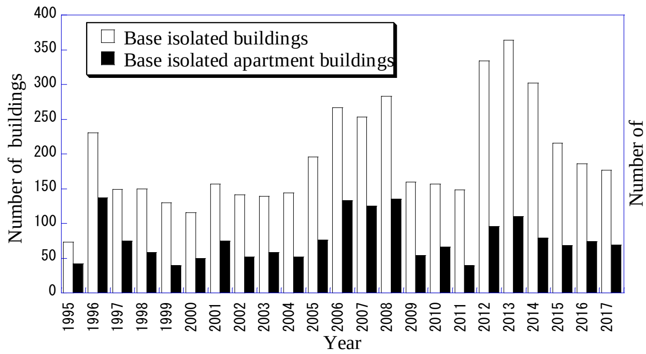

Fig-1 Number of buildings of base isolated buildings constructed in Japan between 1995 and 2017

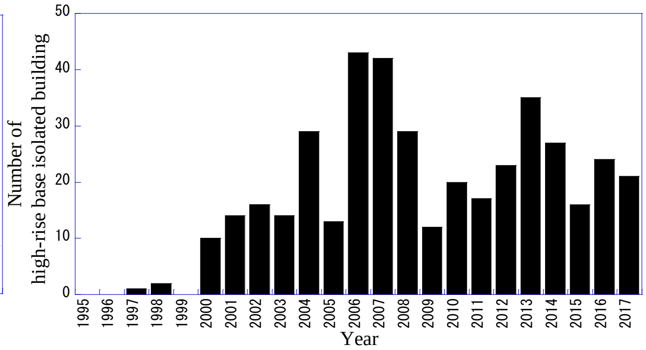

Fig-2 Number of high-rise base isolated building constructed between 1995 and 2017

2. Behavior of base isolated buildings in recent earthquakes in Japan

2.1 Behavior of base isolated buildings in the 2011 Tohoku Earthquake

In the 2013 symposium of the Association of the Japan Society of Seismic Isolation (JSSI), an uplift case with large aspect ratio was reported for a base isolated university office building, located 400km west of the hypocenter. It is important to pay attention to the structural design of large aspect ratio base isolated buildings. After the 2011 Great East Japan disaster, isolator uplift in large aspect ratio base isolated apartment buildings against the long duration of strong ground motion of the great earthquake of M8-9 class is the pressing issue.

2.2 Behavior of base isolated buildings in the Kumamoto Earthquake in 2016

The foreshock and the main shock of the 2016 Kumamoto Earthquake, each with a seismic intensity of 7 (Japan Meteorological Agency (JMA) Seismic Intensity Scale) acted on the buildings of Mashiki Town in Kumamoto Prefecture. Such strong ground motion in two consecutive occasions was not expected and not implemented in the seismic design of the buildings. Ground motion intensity during the 2 - 4 seconds predominant period was high in the 2016 Kumamoto Earthquake. This predominant period is corresponding to the first fundamental period band at the earthquake in base isolated buildings. Scratch pad examination of the movement between the base and the building of a hospital in Aso City during the main shock of the 2016 Kumamoto Earthquake showed a maximum double amplitude of 92 cm and a maximum single amplitude of 46 cm (Img-1-1～Img-1-4).

Img-1-1 Base isolated building of hospital in Aso City

Img-1-2 Multilayered elastomeric isolator of base isolated building of hospital

Img-1-3 Scrach pad of isolation story

Img-1-3 Scratch pad examination of the movement

3. Strong motion record used for earthquake response analysis

3.1. Strong ground motion of the 2011 Tohoku-Chiho Taiheiyo-Oki Earthquake

Table-1 shows records of strong ground motion observed in 39 sites during the 2011 Tohoku-Chiho Taiheiyo-Oki Earthquake, used for the earthquake response analysis.

3.2. Strong motion of the 2016 Kumamoto Earthquake (foreshock and main shock)

Table-2 shows records of strong ground motion observed in 11 sites during the 2016 Kumamoto Earthquake, used for the earthquake response analysis.

3.3. Velocity response spectrum of the horizontal component of the main strong ground motion

Fig-3 shows the velocity response spectrum of the horizontal component of the main strong ground motion of the 2011 Tohoku, and the 2016 Kumamoto Earthquake. In the 2011 Tohoku Earthquake, the velocity response spectrum in IWASE, HAGA, and TUKIDATE is large for less than 1.0 second. On the other hand, the velocity response spectrum in FURUKAWA and INAWASHIRO is large for about 1.5 seconds. Although it is a large earthquake, the velocity response spectrum is different at the plate boundary according to the point where the observed strong motion is observed.

3.4 Acceleration response spectrum of the vertical component of the main strong ground motion

Fig-4 shows the acceleration response spectrum of the vertical component of the main strong ground motion in the 2011 Tohoku, and the 2016 Kumamoto Earthquake. During the Tohoku Earthquake, the acceleration response spectrum of the vertical component in IWASE and HAGA is large for a short period. In the foreshock and the main shock of the Kumamoto Earthquake, the acceleration response spectrum of the vertical component in MASHIKI and MIYAZONO is large for a short period.

Table-1 Strong ground motion of the 2011 Tohoku-Chiho Taiheiyo-Oki Earthquake

No.	Observation site	Com.	Acc.max (cm/s/s)	Vel.max (cm/s)	Dur. (s)	Memo
		H2	562.7	25		Fukushima
1	ONO	H1	633.9	43	300	
		UD	300.8	12		K-NET
		H2	1126.0	43		Fukushima
2	HIRONO	H1	865.2	64	300	
		UD	436.3	18		K-NET
		H2	320.4	27		Fukushima
3	IWAKI	H1	415.2	49	300	
		UD	300.1	13		K-NET
		H2	991.0	42		Fukushima
4	SHIRAKAWA	H1	1339.4	62	300	
		UD	440.7	21		K-NET
		H2	510.2	47		Fukushima
5	SUKAGAWA	H1	614.7	45	300	
		UD	298.1	23		K-NET
		H2	696.4	40		Fukushima
6	KOHRIYAMA	H1	907.8	39	300	
		UD	457.4	25		K-NET
		H2	226.9	45		Fukushima
7	INAWASHIRO	H1	263.8	46	300	
		UD	96.5	15		K-NET
		H2	557.6	37		Ibaraki
8	TAKAHAGI	H1	607.8	53	300	
		UD	495.8	26		K-NET
		H2	1193.6	53		Ibaraki
9	HITACHI	H1	1699.1	64	300	
		UD	1165.7	23		K-NET
		H2	554.5	42		Ibaraki
10	KASAMA	H1	926.3	59	300	
		UD	464.9	18		K-NET
		H2	517.1	39		Ibaraki
11	NAKAMINATO	H1	519.5	49	300	
		UD	411.6	14		K-NET
		H2	1349.6	59		Ibaraki
12	HOKOTA	H1	1378.7	62	300	
		UD	811.2	25		K-NET
		H2	1184.8	54		Iwate
13	ICHINOSEKI	H1	544.2	34	300	
		UD	352.7	18		K-NET
		H2	2094.4	70		Miyagi
14	TSUKIDATE	H1	2710.4	89	300	
		UD	1879.9	38		K-NET
		H2	448.3	62		Miyagi
15	FURUKAWA	H1	577.8	91	300	
		UD	238.8	23		K-NET
		H2	385.1	36		Miyagi
16	ISHINOMAKI	H1	473.5	63	300	
		UD	332.0	18		K-NET
		H2	1453.9	39		Miyagi
17	SHIOGAMA	H1	1643.5	58	300	
		UD	500.8	19		K-NET
		H2	1404.6	54		Miyagi
18	SENDAI	H1	1283.0	82	300	
		UD	290.2	26		K-NET
		H2	321.3	53		Miyagi
19	IWANUMA	H1	411.4	79	300	
		UD	253.9	35		K-NET
		H2	299.0	34		Miyagi
20	KAKUDA	H1	351.8	52	300	
		UD	159.6	15		K-NET
		H2	283.2	21		Tochigi
21	KANUMA	H1	315.0	20	300	
		UD	187.3	10		K-NET
		H2	1063.3	51		Tochigi
22	MOTEGI	H1	973.5	52	300	
		UD	494.2	19		K-NET
		H2	650.9	31		Fukushima
23	NISHIGOU-2	H1	1055.9	34	300	
		UD	1015.8	22		KiK-net
		H2	375.4	22		Fukushima
24	HIRATA-2	H1	379.2	34	300	
		UD	312.5	13		KiK-net
		H2	325.6	40		Fukushima
25	IWAKI-E-2	H1	475.0	73	300	
		UD	230.6	14		KiK-net
		H2	504.1	42		Fukushima
26	MIHARU-2	H1	556.6	41	300	
		UD	360.0	19		KiK-net
		H2	591.7	19		Fukushima
27	MIYAKOJI-2	H1	834.3	63	300	
		UD	729.2	22		KiK-net
		H2	154.5	34		Ibaraki
28	EDOSAKI-2	H1	204.5	51	300	
		UD	236.7	8		KiK-net
		H2	733.3	43		Ibaraki
29	IWASE-2	H1	854.1	57	300	
		UD	815.0	18		KiK-net
		H2	580.1	29		Ibaraki
30	DAIGO-2	H1	586.3	24	300	
		UD	558.4	14		KiK-net
		H2	490.7	28		Ibaraki
31	TAKAHAGI-2	H1	473.2	34	300	
		UD	452.1	11		KiK-net
		H2	503.1	24		Ibaraki
32	HITACHINAKA-2	H1	606.2	32	300	
		UD	341.4	12		KiK-net
		H2	696.4	20		Iwate
33	TAMAYAMA-2	H1	571.1	19	300	
		UD	375.6	14		KiK-net
		H2	327.8	19		Iwate
34	SUMITA-2	H1	366.5	23	300	
		UD	391.1	9		KiK-net
		H2	297.9	26		Miyagi
35	TAJIRI-2	H1	281.3	37	300	
		UD	192.5	15		KiK-net
		H2	313.3	36		Miyagi
36	SHIROISHI-2	H1	313.5	36	300	
		UD	291.0	20		KiK-net
		H2	844.1	46		Miyagi
37	YAMAMOTO-2	H1	846.9	62	300	
		UD	622.2	17		KiK-net
		H2	901.7	65		Tochigi
38	BATOU-2	H1	605.6	36	300	
		UD	245.7	10		KiK-net
		H2	1052.5	66		Tochigi
39	HAGA-2	H1	1048.4	65	300	
		UD	808.08	27		KiK-net

Table-2 Strong ground motion of the 2016 Kumamoto Earthquake (foreshock and main shock)

No.	Observation site	Com.	Acc.max (cm/s/s)	Vel.max (cm/s)	Dur. (s)	Memo
The 2016 Kumamoto earthquake foreshock						
		H2	35.2	3		foreshock,
1	ICHINOMIYA	H1	36.6	3	138	Kumamoto
		UD	35.0	2		K-NET
		H2	215.6	11		foreshock,
2	OHDU	H1	136.0	14	151	Kumamoto
		UD	130.7	5		K-NET
		H2	371.8	61		foreshock,
3	KUMAMOTO	H1	500.3	58	300	Kumamoto
		UD	325.9	14		K-NET
		H2	508.3	16		foreshock,
4	YABE	H1	601.7	21	300	Kumamoto
		UD	95.7	3		K-NET
		H2	492.6	20		foreshock,
5	TOMOCHI	H1	339.6	13	300	Kumamoto
		UD	86.5	5		KiK-net
		H2	214.8	18		foreshock,
6	TOYONO	H1	332.9	31	300	Kumamoto
		UD	228.1	12		KiK-net
		H2	791.9	76		foreshock,
7	MASHIKI	H1	920.6	89	300	Kumamoto
		UD	1399.4	56		KiK-net
		H2	338.9	36		foreshock,
8	MTSUBASE	H1	306.1	49	300	Kumamoto
		UD	220.8	8		JMA
		H2	731.9	122		foreshock,
9	MIYAZONO	H1	813.6	130	120	Kumamoto
		UD	338.2	15		JMA
		H2	516.8	38		foreshock,
10	NISI-KU KASUGA	H1	531.3	61	120	Kumamoto
		UD	261.8	15		JMA
		H2	496.0	34		foreshock,
11	NISHIHARA KOMORI	H1	333.6	32	120	Kumamoto
		UD	180.2	8		JMA
The 2016 Kumamoto earthquake main shock						
		H2	242.7	74		main shock,
1	ICHINOMIYA	H1	373.0	91	300	Kumamoto
		UD	268.5	21		K-NET
		H2	552.4	50		main shock,
2	OHDU	H1	428.2	58	300	Kumamoto
		UD	396.9	53		K-NET
		H2	599.5	57		main shock,
3	KUMAMOTO	H1	667.1	83	300	Kumamoto
		UD	534.3	33		K-NET
		H2	638.3	27		main shock,
4	YABE	H1	769.4	33	300	Kumamoto
		UD	186.6	13		K-NET
		H2	645.9	32		main shock,
5	TOMOCHI	H1	542.8	27	300	Kumamoto
		UD	254.8	9		KiK-net
		H2	452.2	42		main shock,
6	TOYONO	H1	408.0	61	300	Kumamoto
		UD	538.6	24		KiK-net
		H2	625.3	84		main shock,
7	MASHIKI	H1	1183.4	128	300	Kumamoto
		UD	873.4	50		KiK-net
		H2	372.0	52		main shock,
8	MTSUBASE	H1	508.0	79	300	Kumamoto
		UD	313.8	17		JMA
		H2	775.0	96		main shock,
9	MIYAZONO	H1	864.2	180	120	Kumamoto
		UD	668.5	52		JMA
		H2	652.9	53		main shock,
10	NISI-KU KASUGA	H1	503.2	73	300	Kumamoto
		UD	405.2	16		JMA
		H2	718.5	99		main shock,
11	NISHIHARA KOMORI	H1	774.0	247	120	Kumamoto
		UD	531.3	131		JMA

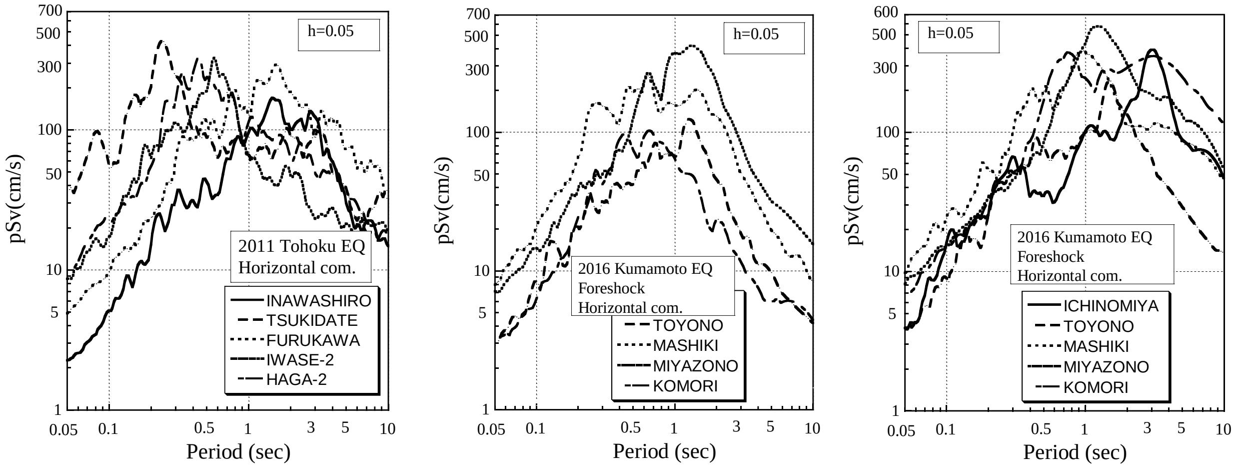

Fig-3 Velocity response spectrum of the horizontal component of the main strong ground motion of the 2011 Tohoku Earthquake and the 2016 Kumamoto Earthquake

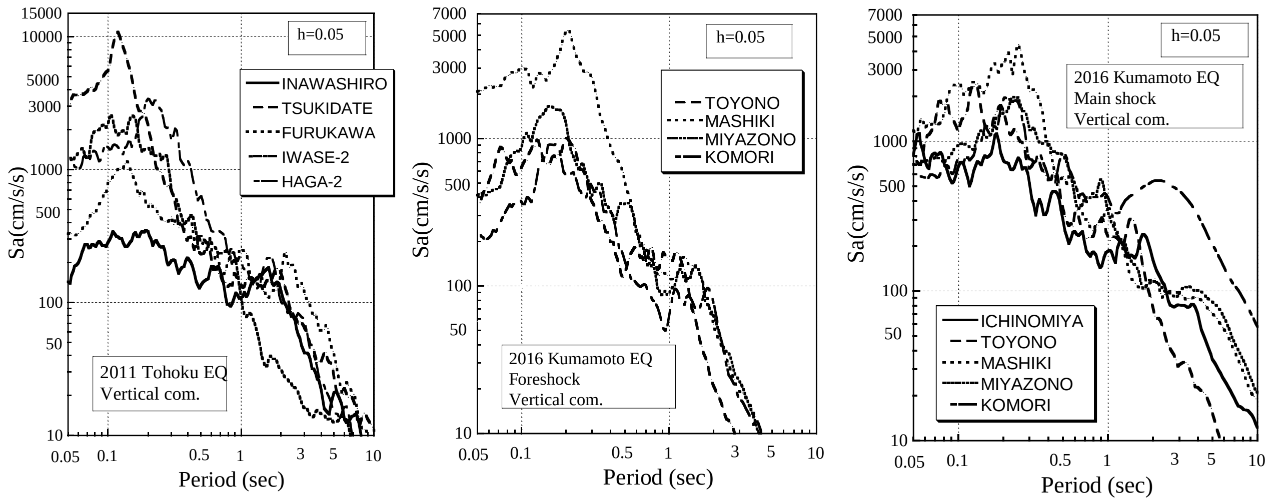

Fig-4 Acceleration response spectrum of the vertical component of the main strong ground motion of the 2011 Tohoku Earthquake and the 2016 Kumamoto Earthquake

3. Building analysis model

3.1. Superstructure

The building analysis model includes the base isolated apartment buildings, and their floor plans in longitudinal direction(X) 7m×5 span, and span direction(Y) 12m×1 span (Fig-5-1). For 12 stories the aspect ratio is 3 (RS12F,H/B=3), for 16 stories the aspect ratio is 4 (RS16F,H/B=4), and for 20 stories the aspect ratio is 5 (RS20F,H/B=5), in span direction, as shown in Fig-5-2. The floor height of each building model is set to H=300cm, and a structural type is assumed to be base isolated apartment buildings of the reinforced concrete construction. The dwelling unit plan is side corridor type, and arranges isolator right under the pillar as shown in Fig-5-1 and Fig-5-2. Fig-5-2 shows the framing elevation in the span direction of RS16F (16 stories, aspect ratio H/B=4). It is assumed that a basic isolation configuration form that installs isolation story between the first floor and the basement, as shown in Fig-5-1 and Fig-5-2.

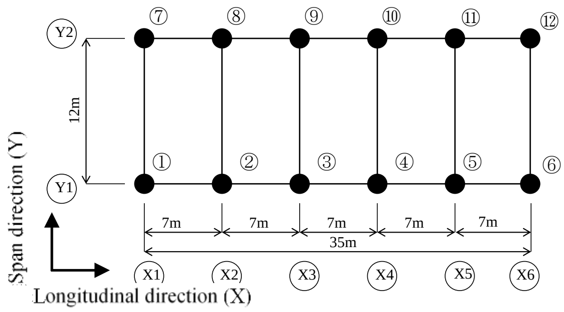

Fig-5-1 Plan of the isolated apartment buildings (RS12F,RS16F,RS20F)

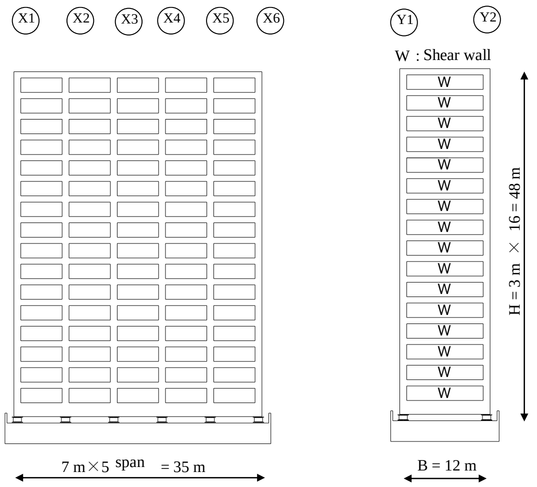

Fig-5-2 Elevation of the isolated apartment buildings(Longitudinal direction (X), Span direction (Y), ex.RS16F)

Table-3 Size of the member of superstructure of RS16F

Floor	Column(mm) Longitudinal	Column(mm) Span	Girder(mm) Longitudinal	Girder(mm) Span	Wall(mm)	Slab(mm)	Superstructure total weight(kN)	Period 1st (superstructure)(s)
13-16	900	700	600×900	600×900	200	200	96,390	0.993
10-12	900	750	600×900	600×900	200	200		
7-9	950	800	600×900	600×900	200	200		Period 1st, γ=100%(isolator)
4-6	1000	850	600×900	600×900	200	200		3.347
1-3	1000	900	600×900	600×900	200	200		Period 1st, γ=200%(isolator)
Founda.	—	—	600×1500	600×2000	200	200		3.476

Table-3 shows the size of the member of superstructure of base isolated apartment buildings (RS16F).

The building model uses the three-dimensional (3D) vibration system by which the mass of the building is concentrated on the beam-column connection. The superstructure is handled as elastic, the damping is type proportional to the rigidity, the damping factor of the superstructure is confronted to the first mode of the three-dimensional(3D) vibration system model, and the damping factor $h_{SH,V}$=2% and isolator story is assumed to be h_{iH}=0% in horizontal direction and h_{iV}=2% in the vertical direction.

The constant acceleration method was applied to the earthquake response analysis technique, and the time interval is set to Δt =0.001 seconds.

In the component of the strong ground motions, the H1 component(strong axis) and the H2 component(weak axis) was calculated from an acceleration orbit that had done the band-pass filter(T=2-6s) of the strong ground motion. The H1 component was input in the span direction(Y), and the H2 component was input for the longitudinal direction (X).

3.2. Member of isolation story

The composition of an isolation story was assumed to be a combination of multilayered elastomeric isolators and steel dampers. Multilayered elastomeric isolators are made from horizontal springs, and the steel dampers are substituted as an energy absorption material.

The isolator diameter (D) is set to become compressive stress σ_L=10N/mm^2 and the 2nd shape factor S_2 = 5. Table-4 shows constants of the multilayered elastomeric isolators and steel dampers. The horizontal characteristic of force-displacement relationship of isolators are assumed elastic, and the period of base isolated building is set to Tf=3.5 seconds.

The steel dampers are set to yield shear force by 5% of superstructure total weight (yield shear coefficient α_s=0.05). The hysteresis characteristics of the horizontal direction of the whole base isolation layer are defined as the bilinear restoration force characteristic by employing a combination of isolators and dampers in Fig-6. The hysteresis characteristics of the vertical direction is treated as elastic with the primary vertical natural period set at 0.15 seconds in consideration to the vertical natural frequency of isolators, the coupled effects of the interacting soil and structure system, and the working design examples. The tensile rigidity of isolators is set at 1/20 of the compressive rigidity and further, set at 1/200 of that upon the tensile stress exceeding 2N/mm^2, and thus defined as having a non-linear form of restoration force characteristics. Fig-7 shows the vertical characteristic of force-displacement relationship in the isolation story.

The Hardening characteristic is not considered about the horizontal characteristic of force-displacement relationship of isolator. The tensile stress was assumed to be an evaluation index in this study. The MSS model is applied to the steel damper.

Table-4 The size of the member of multilayered elastomeric isolator and steel damper

Symbol	Floor	Height (m)	Plan Lx(m)×Ly(m)	Floor height (cm)	Aspect ratio	Corner isolator (D)(mm)	S_2	Normal isolator (D)(mm)	S_2	Total rubber thickness nt_R(mm)
RS12F	12	36	35×12	300	3	700	3.96	950	5.37	6.8×26=176.8
RS16F	16	48			4	800	4.00	1000	5.00	8.0×25=200.0
RS20F	20	60			5	900	3.73	1200	4.98	6.7×36=241.2

Symbol	Floor	Height (m)	Plan Lx(m)×Ly(m)	Floor height (cm)	Aspect ratio	Period of isolator Tf(sec)	Elastic limit displacement of damper δy(mm)	Yield shear coefficient of damper α_s
RS12F	12	36	35×12	300	3	3.5	30	0.05
RS16F	16	48			4			
RS20F	20	60			5			

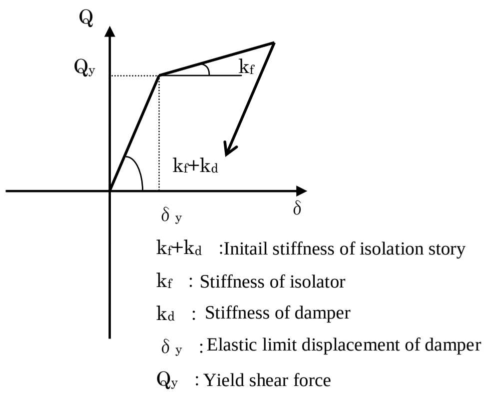

Fig-6 Horizontal characteristic of force-displacement relationship of isolation story

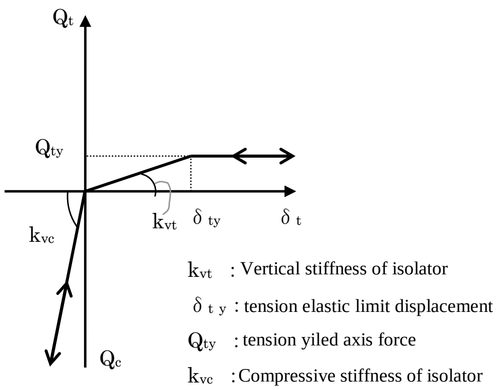

Fig-7 Vertical characteristic of force-displacement relationship of isolation story

4. Uplift of isolators of base isolated high-rise buildings

4.1. Isolator tensile stress of earthquake response by strong motion in the 2011 Tohoku Earthquake

Fig-8 shows isolator tensile stress of earthquake response by strong motion in the 2011 Tohoku Earthquake. Fig-8 also shows the relation of the shear strain and tensile stress on isolator uplift. The strong motion of the 2011 Tohoku Earthquake exceeded tensile stress by 1N/mm^2, which apparently exceeded the pulling allowance of the isolator.

Extensive shearing strain and isolator pulling in base isolated buildings was observed in various locations after the 2011 Tohoku Earthquake. Extensive shearing strain is caused in the isolator when a strong motion acts on base isolated high-rise buildings, causing the isolator to be pulled out.

4.2. Isolator tensile stress of earthquake response by strong motion in the 2016 Kumamoto Earthquake

Fig-9 shows the isolator tensile stress of earthquake response by strong motion in the 2016 Kumamoto Earthquake. Strong motion exceeded tensile stress by 1N/mm^2, and it can be seen that, similar to the case in the 2011 Tohoku Earthquake, the pulling allowance of the isolator was exceeded.

Isolator tensile stress is larger than that of the strong motion of the 2011Tohoku Earthquake because the hypocenter distance is short due to the Kumamoto Earthquake being an intraplate earthquake. The isolator tensile stress tends to grow with the number of stories (aspect ratio) in base isolated high-rise buildings.

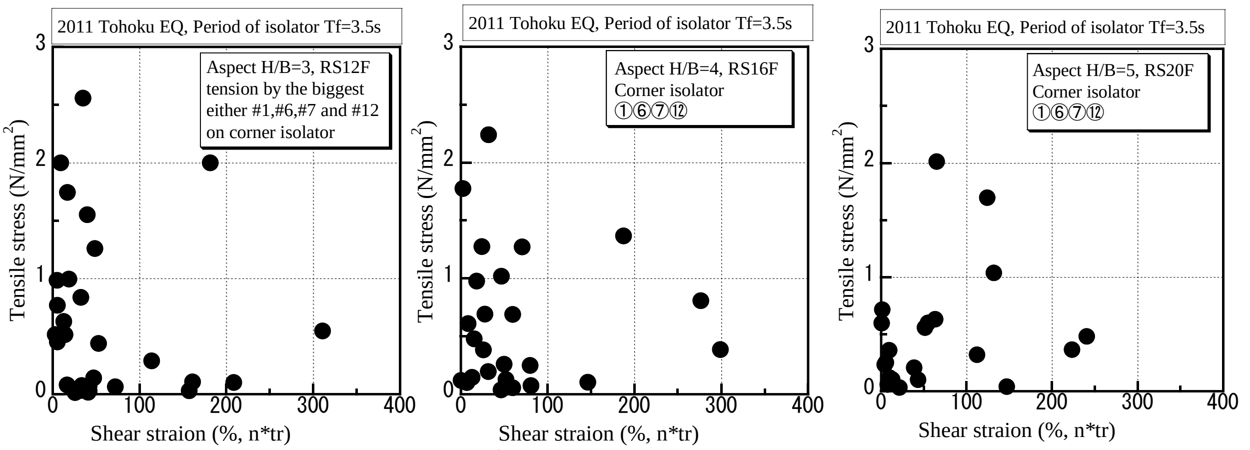

Fig-8 Relation of the shear strain and tensile stress on isolator by strong motion in 2011 Tohoku Earthquake

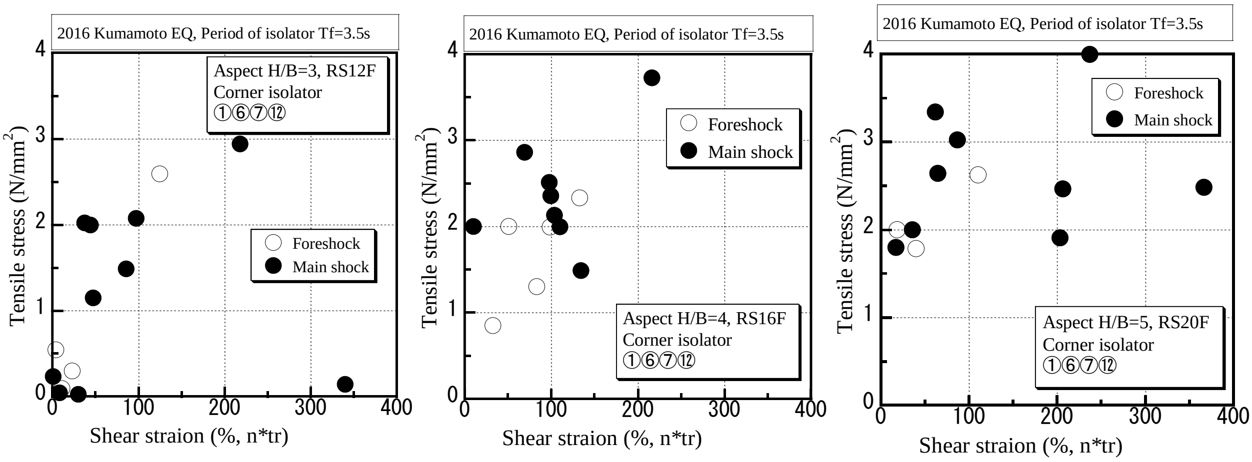

Fig-9 Relation of the shear strain and tensile stress on isolator by strong motion in 2016 Kumamoto Earthquake

4.3. Quantitative evaluation of the effect of horizontal and vertical motions on isolator uplift

Drawing on the above, the earthquake response properties of base isolated high-rise buildings were reviewed to identify the time difference in the response axial forces acting on isolators in the main moving parts due to the horizontal and vertical motions. Moreover, through the study of the simultaneous input of the three components of seismic motion, two horizontal and one vertical, and the sole input of two horizontal components, the effects of horizontal motions on isolator uplift were defined as “horizontal motion efficiency,” and those of vertical motion on isolator uplift, defined as “vertical motion efficiency.” By analyzing the results in terms of these factors, it was possible to quantitatively evaluate the effect of the horizontal motions and the vertical motion on the isolator uplift.

Isolator pulling was caused in the 2011 Tohoku Earthquake, and the 2016 Kumamoto Earthquake because vertical motion efficiency is about 1.0 (Fig-10, Fig-11). Vertical motion efficiency decreases as the number of stories increases, leading to an increase of horizontal motion efficiency.

Comparing Fig-10 and Fig-11, in the strong motions of the 2016 Kumamoto Earthquake of Fig-11, the horizontal motion efficiency of the 12 story base isolated buildings can be considered as large. Vertical motion efficiency grows as the number of stories increases and horizontal motion efficiency increases without the number in Fig-10 decreasing. The strong ground motion with a large evaluation of both the vertical motion efficiency and the horizontal motion efficiency exists for the 20 stories base isolated high-rise building.

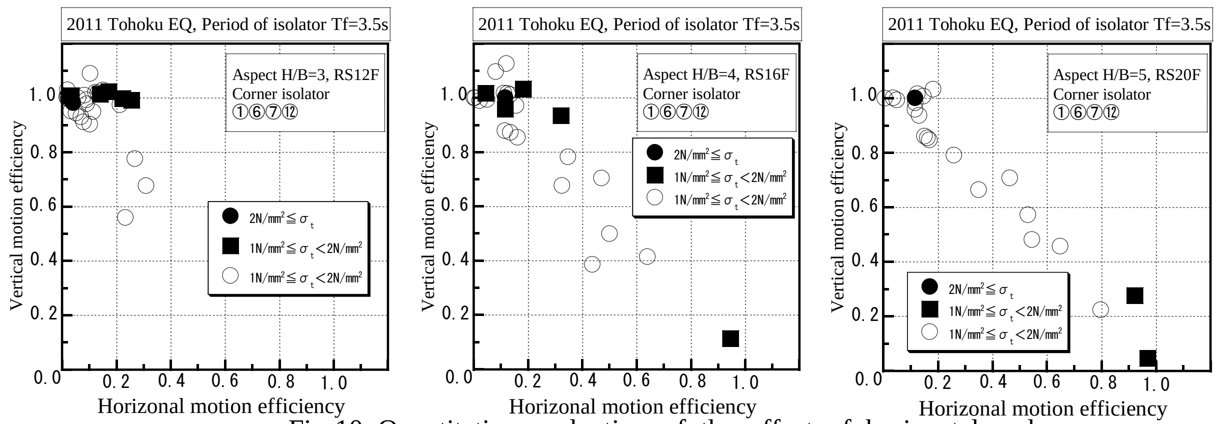

Fig-10 Quantitative evaluation of the effect of horizontal and vertical motion on isolator uplift by strong motion in 2011 Tohoku Earthquake

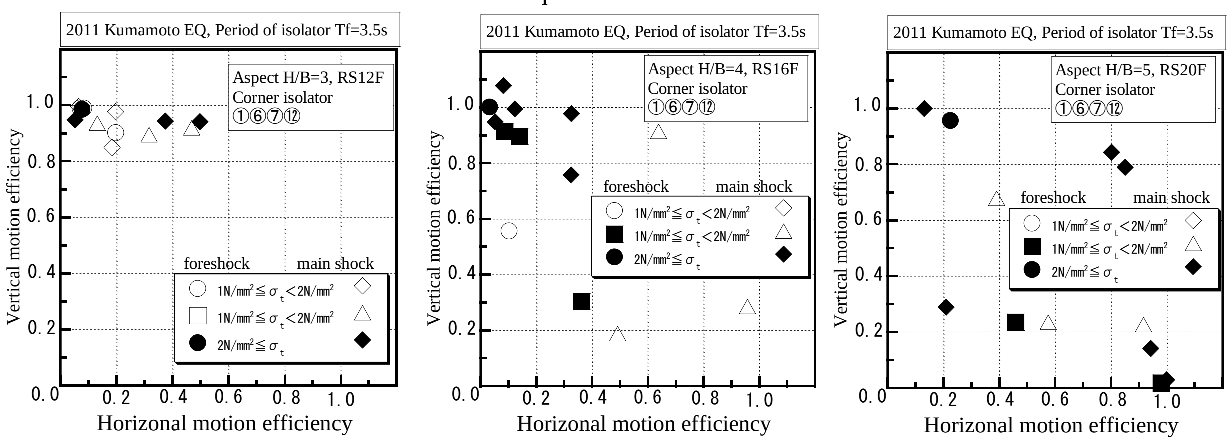

Fig-11 Quantitative evaluation of the effect of horizontal and vertical motion on isolator uplift by strong motion in 2016 Kumamoto Earthquake

5. Conclusions

The earthquake response analysis in a large aspect ratio of base isolated high-rise buildings was performed by using strong ground motion data from the 2011 Tohoku and the 2016 Kumamoto Earthquake.

The fluctuating stress on corner isolators in base isolated high-rise buildings with an aspect ratio of 3 or higher when subjected to seismic motions are larger than normal isolators, and as the aspect ratio increases the fluctuating axial force associated with the overturning moment due to the horizontal motion increases, so the maximum tensile stress tends to increase.

In examples of recently designed base isolated high-rise buildings with large aspect ratios, it was found that in some cases the tensile stress of corner isolators in base isolated high-rise buildings with aspect ratios of 3 or higher exceeded a tensile stress of $1N/mm^2$, which is the target value for performance based design, and the maximum tensile stress exceeded $2N/mm^2$.

6. References

[1] Ikeda Y. and Nagahashi S. (2011) : The earthquake response characteristics of characteristics of base isolated high-rise buildings subject to scenario earthquakes in japan and the effects of aspect ratio on their responses, A study on the effects of simultaneous action of horizontal and vertical ground motion on the earthquake response characteristics of base isolated high-rise buildings part 3, J.Struct. Constr. Eng., AIJ, Vol.76 No.660, pp.281-290, Feb., 2011

[2] AIJ (2018) : Report on the damage investigation of the 2016 Kumamoto Earthquake, Jun., 2018

[3] Kasai K : Analysis of earthquake response record in up-to-date structural building, Approach of response control building in the future, -problem of the 2011 Tohoku-Chiho Taiheiyo-Oki Earthquake-, Association of the Japan Society of Seismic Isolation (JSSI), Feb., 2013

[4] Takayama M. (1995) : Ultimate capacity of natural rubber bearings used in seismic isolation system, AIJ J. Technol. Des. No.1, pp.160-165, Dec., 1995

[5] Muramatsu Y., Nishikawa I., Kawabata I., Takayama M. and Kimura Y. (2001) : Tensile property of Large-sized natural rubber bearing, AIJ J. Technol. Des. No.12, pp.53-56, Jan., 2001

[6] AIJ (2001) : 2. Isolator, Recommendation for the design of base isolated buildings, pp.35-39, Sep., 2001

[7] Mori T., Nakamura M., Murota N., Kitamura H. and Sato T. (2015) : Evaluation of tensile characteristics of rubber bearings to design seismically isolated structure by design limit value of tensile strain, J.Struct. Constr. Eng., AIJ, Vol.80 No.718, pp.2021-2031, Dec., 2015

